Sorption and Desorption of Tetrachloroethylene in Fluoropolymers: Effects of the Chemical Structure and Crystallinity

M. S. Hedenqvist,[1] J. E. Ritums,[1,2] M. Condé-Brana,[2]* G. Bergman[2]

[1] *Department of Fibre and Polymer Technology, Royal Institute of Technology, S-100 44 Stockholm, Sweden*
[2] *Swedish Corrosion Institute, Kräftriket 23A, SE-104 05 Stockholm, Sweden*

Received 9 October 2001; accepted 31 May 2002

ABSTRACT: In 18 fluoropolymers with different repeating-unit structures and crystallinities, the solubility, diffusivity, and permeability at 70°C of a polarizable nonpolar solute (tetrachloroethylene) were studied. The transport properties were mostly controlled by the polarity of the polymer and to a lesser degree by the polymer crystallinity. The highest permeability was observed in the dipole-containing ethylene–chlorotrifluoroethylenes because of their high tetrachloroethylene solubility. The lowest permeability was observed in the hydrogen-bonding poly(vinylidene fluoride) polymers because of the combination of low solute solubility and solute diffusivity. The tetrachloroethylene diffusivity was solute-concentration-dependent, and sorption curves were S-shaped, indicating that the solute surface concentration was time-dependent. The rate at which the surface concentration approached the saturation level was proportional to the product of Young's modulus, the square of the thickness of the dry polymer, and the logarithm of the solute diffusivity. Data for the water-hyperbranched polymer and limonene–polyethylene conformed to the same relationship. Therefore, this provides a new tool for predicting the solute-surface-concentration time dependence from data obtained by independent measurements. © 2002 Wiley Periodicals, Inc. J Appl Polym Sci 87: 1474–1483, 2003

Key words: diffusion; fluoropolymers; strength

INTRODUCTION

Fluoropolymers are used extensively in severe environments, including linings on structures of steel or fiber-reinforced plastics (FRPs). Their excellent thermal and chemical resistance makes them attractive as protection on process components in the pulp and paper, chemical, petrochemical, pharmaceutical, and electronics industries. In the production of chlorine by modern membrane technology, fluoropolymer-lined FRP pipes are used for transporting spent brine and hot and wet chlorine gas, for example.[1,2]

Even though fluoropolymers have been used for a long time in these environments, little is known about their long-term performance in severe environments. A knowledge of the chemical–polymer interactions, including the sorption and desorption characteristics of these polymers, is important for assessing the long-term properties of polymer products. Only a few articles have reported sorption and desorption data.[3,4] Although the lining itself appears to be unaffected by the chemical, the underlying matrix may be attacked because the chemical may diffuse rapidly through the lining. An FRP pipe exposed to outlet warm brine for 5 years had a degraded layer, consisting of a chlorine-rich powder, next to the fluoro-ethylene copolymer (FEP) lining, although the lining appeared unaffected. In other circumstances, the lining may swell readily in contact with the chemical, which results in swelling-induced mechanical stresses.[5] These stresses, developing during the sorption of the chemical, may cause debonding between the matrix and the lining. The swelling-induced mechanical stresses may also cause environmental stress cracking.[6] In addition, cracks can develop during chemical desorption from the lining (e.g., during a shutdown in production) because tensile stresses then develop in the surface.

This study explored the sorption and desorption characteristics of a broad range of fluoropolymers exposed in tetrachloroethylene (TCE), a symmetrical and, therefore, nonpolar chemical. TCE was chosen because it represents a large and important group of chemicals (readily polarizable, although their gas-phase/dipole moment is zero) that frequently come into contact with fluoropolymers. Another goal was to determine whether the differences in the sorption behaviors of the different polymers could be explained from the differences in their mechanical response.

Correspondence to: M. S. Hedenqvist (mikaelhe@polymer.kth.se).

**Present address:* Habia Cable AB, Box 5075, SE-187 05 Täby, Sweden.

Contract grant sponsors: Swedish Foundation for Strategic Research; Plastics Research Programme of the Swedish Corrosion Institute.

Journal of Applied Polymer Science, Vol. 87, 1474–1483 (2003)

The fluoropolymers used in this study were poly(tetrafluoroethylene) (PTFE) homopolymers, including PTFEs slightly modified with perfluoropropylvinylether (PFPVE), and copolymers of tetrafluoroethylene with PFPVE, perfluoromethylvinylether (PFMVE), or hexafluoropropylene (HFP; Fig. 1). The latter three are called PFA, MFA, and FEP polymers. In addition, ethylene–tetrafluoroethylene (ETFE), ethylene–chlorotrifluoroethylene (ECTFE), and poly(vinylidene fluoride) (PVDF) were included (Fig. 1).

EXPERIMENTAL

Materials

The characteristics of the materials are presented in Table I. These polymers were kindly supplied by Ausimont S.p.A. (Bollate, Italy). The PTFE-based samples, containing no copolymer or less than 1 mol % were called PTFE materials. TCE was a 99.5% purity grade (VWR International, Stockholm, Sweden; ρ_1 = 1110 kg m^{-3}). The PFA, MFA, FEP, ETFE, ECTFE, and PVDF materials were compression-molded into 1.35–1.5-mm-thick plates at 350, 370, 320, 300, 260, and 200°C, respectively. The samples were preheated between the plates for 5 min without pressure and then exposed to a pressure of 4 MPa for 2 min. The cycle was ended by the water cooling of the plates for 2 min with the pressure maintained at 4 MPa. The PTFE materials were sintered into 1.06–1.2-mm-thick skived tapes at 370°C for 36 h.

TABLE I
Characteristics of Samples

Sample	Copolymer[a]	X[b] (mol %)	Melting point (°C)	Polarity[c]
PTFE1	—	—	331	1
PTFE2	PFPVE	0.1–0.2	332	1
PTFE3	PFPVE	0.1–0.2	331	1
PTFE4	PFPVE	0.1–0.2	330	1
PFA1	PFPVE	2.4	306	2
PFA2	PFPVE	2.4	306	2
PFA3	PFPVE	2.2	308	2
PFA4	PFPVE	2.2	308	2
MFA	PFMVE	4.5	286	2
ETFE	—	—	268	3
FEP1	HFP	7.2	261	2
FEP2	HFP	7.3	260	2
ECTFE1	—	—	241	4
ECTFE2	—	—	228	4
PVDF1	HFP	2.0	158	5
PVDF2	—	—	170	5
PVDF3	—	—	174	5
PVDF4	—	—	167	5

[a] PTFE modified with either PFPVE, PFMVE, or HFP.
[b] The copolymer contents of the PFA, MFA, and FEP polymers were estimated from melting-point data with information in ref. 24. Other data came from the supplier.
[c] (1) Nonpolar, (2) nearly nonpolar, (3) weak dipolar and hydrogen bonds, (4) dipoles, and (5) hydrogen bonds.[3, 4]

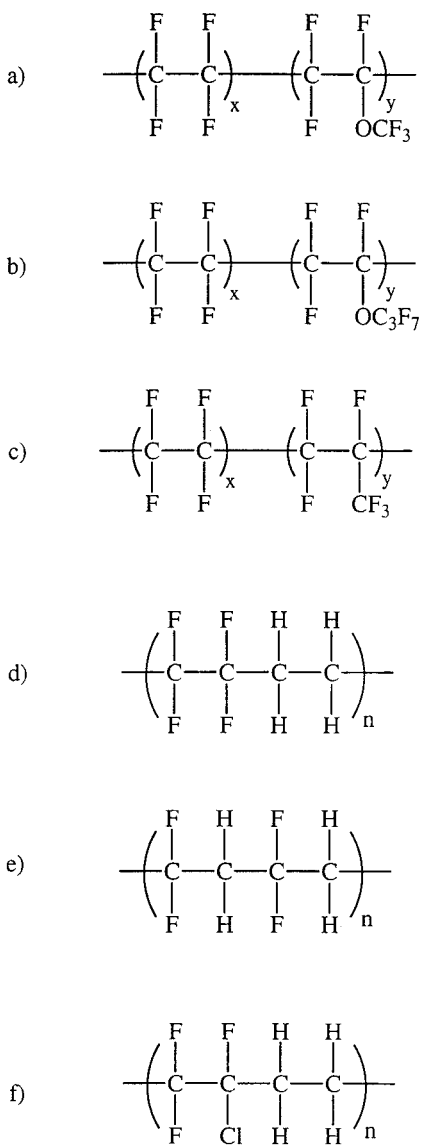

Figure 1 Chemical structures of (a) MFA, (b) PFA, (c) FEP, (d) ETFE, (e) PVDF, and (f) ECTFE.

Sorption and desorption measurements

The sorption experiment was performed by the immersion of the specimen at 70°C in a bottle containing the liquid. The mass increase was recorded by the intermittent weighing of the surface-dried sample with a Sartorius balance. The desorption experiment was performed on the solute-saturated specimen by it being placed in a 70°C warm-air-conditioned heat chamber. The mass decrease was recorded by the intermittent weighing of the specimen with the Sartorius balance. The gravimetric data indicated that no residual TCE was left in the specimens after desorption.

Differential scanning calorimetry

The melting endotherms of the polymers were obtained by the heating of 5-mg samples (±1 mg) at a rate of 10°C min^{-1} with a temperature- and energy-calibrated Mettler–Toledo DSC 820 instrument.

Tensile testing and stress relaxation

The stress–strain and stress-relaxation properties were measured on 25-mm-long, dumbbell-shaped specimens (thickness = 1.35–1.5 mm, width of narrow section = 2.2 mm, and gauge length = 22 mm) at 70°C and 40% relative humidity, with an Instron 5566 testing instrument recording the strain between gauges. The stress–strain properties were recorded at a strain rate of 500 mm min^{-1}, and Young's modulus (E) was calculated as the initial slope of the stress–strain curve. The stress relaxation was obtained on specimens rapidly strained to a 4% engineering strain, with a ramp time of less than 1 s.

Contact-angle measurements

The contact-angle measurements were performed with a Ramé Hart goniometer and the sessile drop technique. Deionized water was used, and the water drop was applied with a hollow needle. The reported values are the averages of six measurements on different drops. The advancing contact angles were obtained by the needle being kept in the water droplet after it was positioned on the surface and by the careful addition of more water until the advancing angle appeared to be a maximum.

THEORY

For the plate geometry, Fick's second law of diffusion[7] is given as follows:

$$\frac{\partial C}{\partial t} = \frac{\partial}{\partial x}\left(D(C)\frac{\partial C}{\partial x}\right) \tag{1}$$

where D is the diffusivity ($cm^2\ s^{-1}$), x is the distance (cm), and C (g cm^{-3}) is the penetrant concentration. Only half the plate thickness (L) was considered, and the inner boundary coordinate can be described as an isolated point:

$$\left(\frac{\partial C}{\partial x}\right)_{x=L/2} = 0 \tag{2}$$

The outer boundary condition is described as follows:

$$\left[\tau_c\frac{\partial C}{\partial t}\right]_{x=0} + (C - C_\infty)_{x=0} = 0 \tag{3}$$

where C_∞ is the final concentration and τ_c is the surface-concentration relaxation time. During desorption, the surface concentration was kept at zero because solute surface evaporation was rapid in comparison with solute bulk diffusion, as indicated by straight desorption curves at short times. The concentration-dependent diffusivity [$D(C)$] can be expressed as follows:[8]

$$D(C) = D_{co}e^{\alpha_D C} \tag{4}$$

where D_{co} is the zero-concentration diffusivity and α_D is the plasticization power. This equation has been used extensively, and it has been shown that it fits diffusivity data well.[9,10] Additionally, it can be derived and motivated by the application of free-volume theories.[11,12] Equation (1), combined with eq. (4) and the appropriate boundary conditions previously given, was solved by a multistep backward implicit method described in detail by Hedenqvist and coworkers.[5,13]

RESULTS AND DISCUSSION

Figure 2(a–f) presents sorption–desorption curves for TCE in one material from each series. The shapes of the sorption and desorption curves were similar for most materials, except for ECTFE. As shown in Figure 2(e), it was not possible to fit the entire sorption curve for ECTFE. The sorption and desorption curves intersected each other for all the materials, and this indicates that the diffusion coefficient of TCE was concentration-dependent.[7] All sorption curves were sigmoidal in shape, and this indicates that the surface concentration was time-dependent.[5,14,15] A time-dependent surface concentration during sigmoidal sorption was recently verified by infrared spectroscopy.[16]

The mass crystallinity was estimated from the ratio of the measured heat of melting (ΔH_f) and the heat of melting of 100% crystalline polymer (ΔH_f^o). For PTFE, PFA, MFA, and FEP, ΔH_f^o was taken from the homopolymer (82 J/g[17]). ΔH_f^o values for the PVDF and ECTFE series were 104.6[18] and 146 J/g,[19] respectively. For ETFE, ΔH_f^o was 128 J/g, which was estimated under the assumption that the polymer consisted of 50 mol % PTFE (82 J/g) and 50 mol % linear polyethylene (293 J/g).[20]

The volume fraction of liquid TCE in the amorphous polymer component [$v_1{}^a = v_1/(1 - w_c)$] are shown in Figure 3. v_1 is the TCE volume fraction, and the mass crystallinity (w_c) was used in the calculations, rather than the volume crystallinity, because the crystal and amorphous densities were not available for all the polymers. This should, however, have a small impact on the trends in solubility. According to the hypothesis that the crystals were impenetrable to TCE, the variations in the solubility between the different

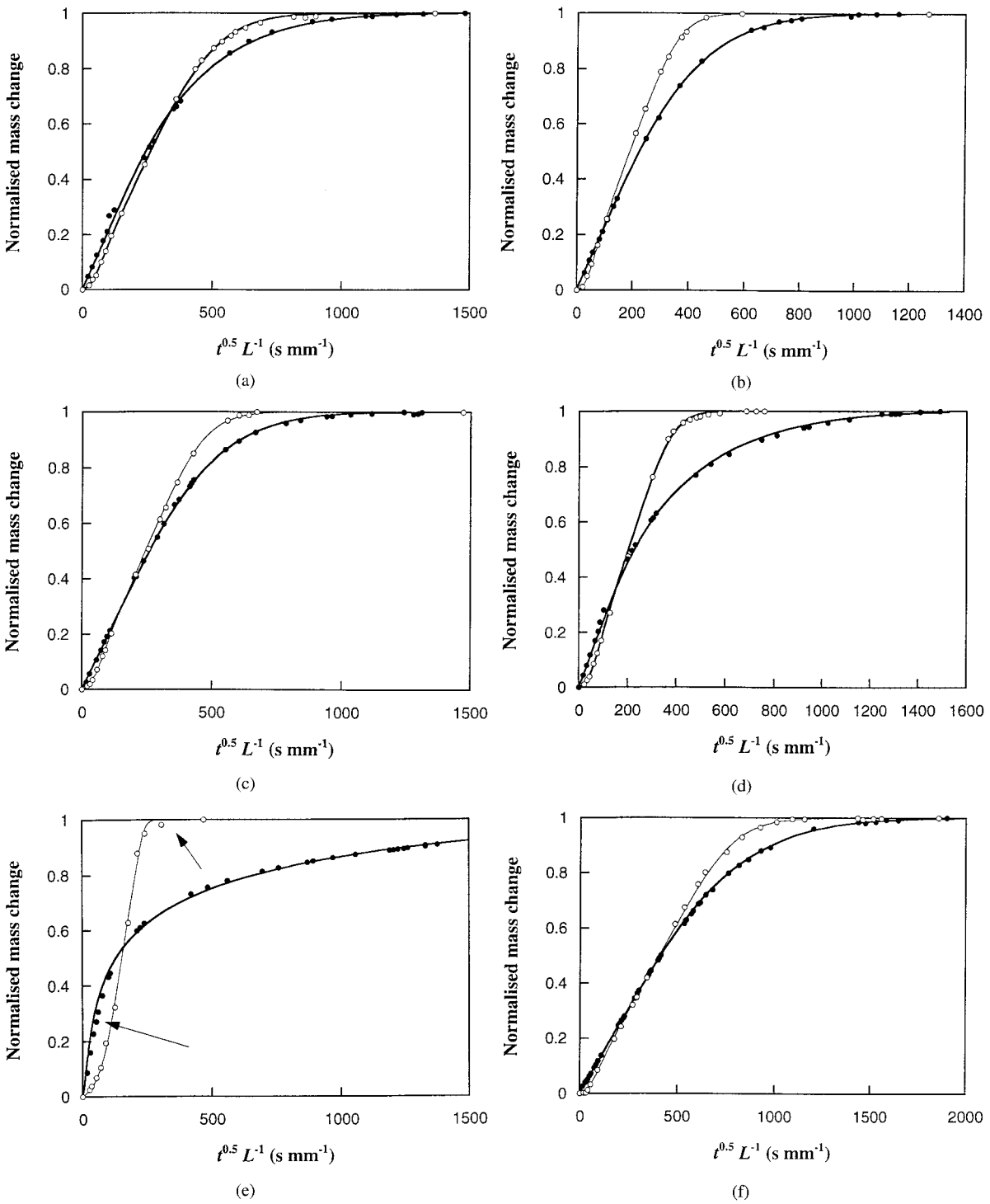

Figure 2 Experimental (○) sorption and (●) desorption curves for TCE in (a) PTFE2, (b) PFA1, (c) FEP2, (d) ETFE, (e) ECTFE1 (the arrows indicate the points at which the model was unable to fit the experimental values), and (f) PVDF1. The solid lines represent best fits by the numerical method [eqs. (1)–(4)]. t is the time, and L is the thickness.

polymers should reflect variations of the physics and chemistry of the amorphous components. The solubility of TCE was highest in the two polymers that formed dipoles with it, that is, ECTFE and ETFE. The amorphous solubility was low and basically constant within the hydrogen-bonding PVDF series. For the nonpolar or nearly nonpolar polymers, the amorphous solubility increased slightly with increasing crystallinity. There was no obvious explanation for this odd behavior; however, the presence of the comonomers (PFPVE, PFMVE, and HFP) evidently led to a slight lowering of the TCE amorphous solubility.

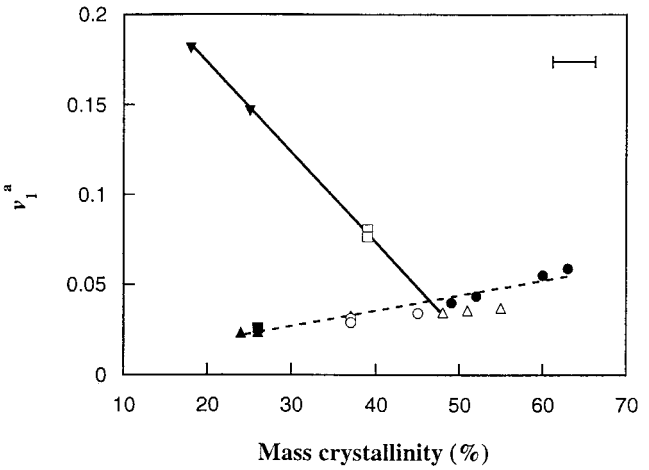

Figure 3 Sorbed volume fraction of liquid TCE in the amorphous polymer component as a function of the mass crystallinity of (●) PTFE, (○) PFA, (■) MFA, (▲) FEP, (□) ETFE, (△) PVDF, and (▼) ECTFE. The solid line represents the trend in the TCE solubility for the groups ECTFE, ETFE, and PVDF. The broken line represents the trend in the TCE solubility for the groups PTFE, PFA, MFA, and FEP. The error in the TCE volume fraction values was estimated to be ±5% of the value. The error bars in this and the following figures are rough estimates.

The general trends in TCE solubility could very well be rationalized in terms of the Hansen solubility parameters (Table II). It was here assumed that the solubility parameters and their relative sizes, which were determined at ambient temperature, were temperature-independent. This is a common and accepted approach, although it should be stated that the hydrogen-solubility parameter component decreased slightly faster with increasing temperature than the dispersion and polar components.[21] Unfortunately, it was not possible to obtain solubility parameters for all the polymers. As expected, the TCE amorphous solubility increased with a decreasing solubility parameter distance (Table II). The high solubility in ECTFE could be explained by the fact that the polar solubility parameter was similar to that of TCE. In the same way, the low solubility of TCE in PVDF was explained by the large difference in the hydrogen-bonding solubility parameter. ETFE, which partly resembled ECTFE and partly resembled PVDF, should have solubility parameter values intermediate between the values for the two polymers. It may also be expected that PFA, MFA, and FEP solubility parameters would be close to those of PTFE.

The TCE D_{co} value is given as a function of the crystallinity in Figure 4. First, the variation in the diffusivity for the different fluoropolymers was not very large. The diffusivity decreased linearly with increasing crystallinity for the PTFE/PFA/MFA series. Therefore, the crystals were impenetrable. D_{co} also decreased with increasing crystallinity within the PVDF series. FEP had a lower diffusivity than MFA at the same crystallinity. The reason for this is not obvious. The lowest TCE D_{co} value was obtained in the dipole-containing polymer (ECTFE). Therefore, dipoles (ECTFE) were more effective than hydrogen bonds (PVDF) in retarding the TCE diffusional jumps, and dipoles between polymer–polymer segments and solute–polymer segments were effective in lowering the diffusion rate of an easily polarizable solute (TCE). Interestingly, the D_{co} value of the semidipolar/semihydrogen-bonding polymer (ETFE) was closer to that of PVDF than to that of ECTFE.

The diffusivity of one polymer in each group, calculated from eq. (4), is given as a function of the TCE concentration in Figure 5. The magnitude of the concentration dependence (α_D, the steepness of the curves) among the polymers was small. The highest and lowest concentration dependencies were observed for PTFE and ETFE. By comparing the slopes in Figure 5, one could conclude that the very pronounced S-shaped sorption curve of ECTFE [Fig. 2(e)] could be explained by the large TCE solubility in this polymer and not by an extraordinarily high value of α_D. The diffusivity of ECTFE from dry to wet increased by more than five orders of magnitude!

Most practical problems of permeability in linings relate to a steady-state flow of the solute through the material. The flow rate in a plate, in which the diffusivity is highly concentration-dependent, can be obtained by the definition of an effective permeability:

$$\bar{P} = \bar{D}C_\infty \tag{5}$$

where the average diffusivity is[7]

$$\bar{D} = \frac{1}{C_\infty}\int_0^{C_\infty} D_{co}\, e^{\alpha_D C}\, dC \tag{6}$$

TABLE II
Hansen Solubility Parameters[21] (MPa)$^{0.5}$

Material	∂_d^a	∂_p^b	∂_h^c	∂^d	R_a^e	v_1^{af}
TCE	18.3	5.7	0	19.2		
PTFE[g]	15	1.4	1	15.1	7.9	0.05
ECTFE	18.2	7.9	4.8	20.4	5.3	0.16
PVDF	17	12.1	10.2	23.2	12.3	0.035

[a] Dispersion solubility parameter.
[b] Polar solubility parameter.
[c] Hydrogen-bonding solubility parameter.
[d] The average solubility parameter.
[e] Solubility parameter distance.
[f] The saturation volume fraction of TCE in the amorphous polymer component. Values were averages for the whole series of each polymer type.
[g] Solubility parameters were taken as averages from refs. 21 and 25.

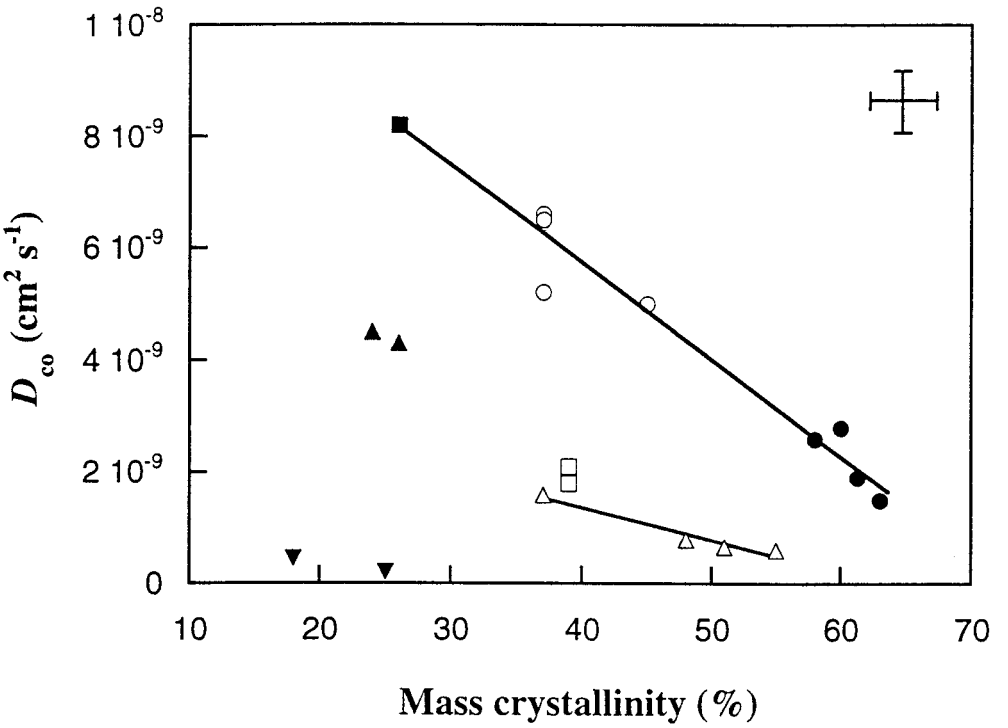

Figure 4 TCE D_{co} as a function of the mass crystallinity (●) PTFE, (○) PFA, (■) MFA, (▲) FEP, (□) ETFE, (△) PVDF, and (▼) ECTFE. The lines illustrate the trend in D_{co} for the PTFE/PFA/MFA and PVDF series.

where C_∞ is the saturation concentration of TCE in the polymer. It corresponds to the case in which the surface concentration of TCE is at the saturation level on the liquid TCE side and zero on the outer polymer surface. The effective permeability as a function of the crystallinity is given in Figure 6. The effective permeability decreased only mildly with increasing crystallinity for the PTFE/PFA/MFA series and also within the PVDF series. The worst barrier to TCE was ECTFE, explained by the high dipolar affinity between TCE and ECTFE, resulting in a high TCE solubility (Fig. 3).

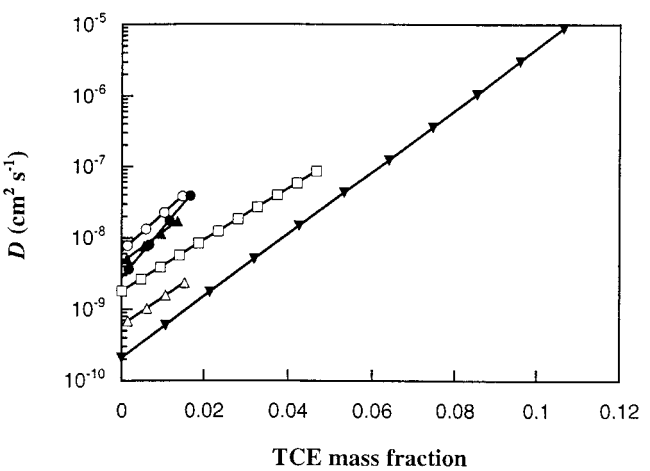

Figure 5 TCE concentration dependence calculated according to eq. (4) for (●) PTFE3, (○) PFA1, (▲) FEP1, (□) ETFE, (△) PVDF3, and (▼) ECTFE1.

The best barrier to TCE was PVDF because of the low solubility and low diffusivity of TCE in this polymer. Evidently, for a nonpolar (zero gas-phase/dipole moment) but polarizable solute, a hydrogen-bonding polymer (PVDF) provides the best protection. The chemical effects (polarity) seemed to be more important than the degree of crystallinity.

An attempt was made to determine whether a single parameter could be used to predict the TCE diffusivity

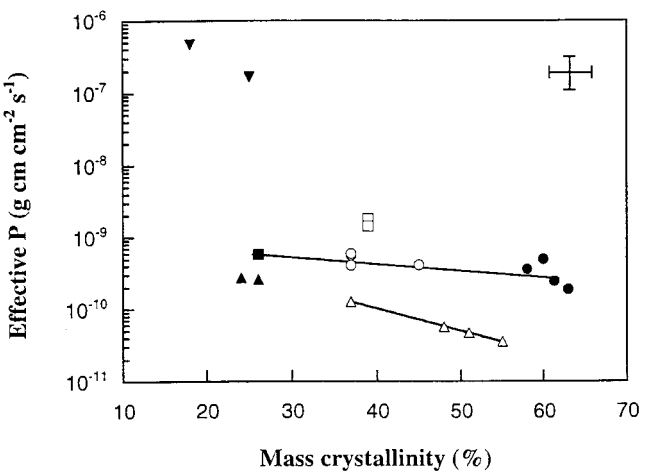

Figure 6 TCE effective permeability as a function of the mass crystallinity of (●) PTFE, (○) PFA, (■) MFA, (▲) FEP, (□) ETFE, (△) PVDF, and (▼) ECTFE. The lines illustrate the trends in the effective permeability for the PTFE/PFA/MFA and PVDF series.

for any fluoropolymer. The only detectable trend was observed when the TCE D_{co} values for all fluoropolymers were plotted together as a function of the water advancing contact angle (Fig. 7). Although the contact angle was affected by many parameters, it seemed that a lower contact angle corresponded to a higher polarity or hydrogen-bonding capacity, which, in turn, yielded a lower value of D_{co}. The fact that the only parameter that united all the fluoropolymers was the contact angle strengthened the earlier observation that the chemistry was more important than the degree of crystallinity.

Solute-induced stresses develop during solute sorption in swelling systems and complicate the calculation of solute diffusivity from sorption data. This phenomenon is complex, but it has been shown that it is possible to describe the whole sorption curve by the consideration of a time-dependent solute surface concentration:[5,8–10,14,22]

$$C = C_i + (C_\infty - C_i)(1 - e^{-\frac{t}{\tau_c}}) \quad (7)$$

It is here assumed that the solute surface concentration reaches a value (C_i) instantaneously, which yields an immediate strain of the polymer. The surface concentration thereafter increases gradually toward a final value (C_∞) at a rate determined by the surface stress-relaxation time (τ_c). Equation (7) is readily derived from eq. (3). This process is schematically illustrated in Figure 8. The thickness of the plate increases more rapidly than its cross section during the early stages of sorption (stage I), whereas the opposite trend is observed during the later stages (stage II).[5,15,23] This is explained by the fact that, during stage I, compressive stresses are exerted by the still dry plate core on the plate surface, leading mainly to one-dimensional swelling. At the onset of stage II, which is characterized by three-dimensional swelling, the solute reaches

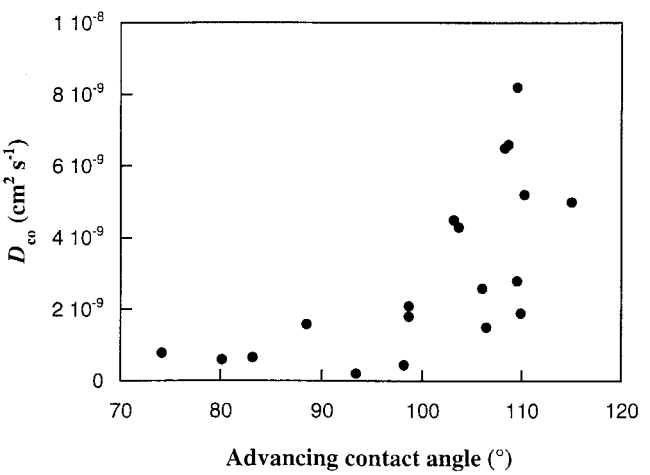

Figure 7 TCE D_{co} values for all the fluoropolymers as a function of the water advancing contact angle.

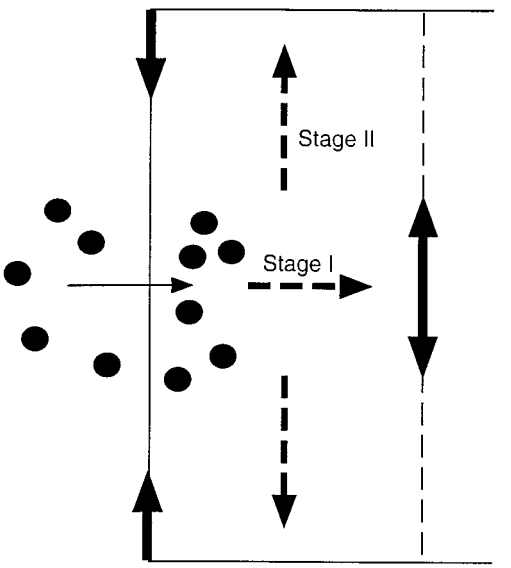

Figure 8 Schematic illustration of the solute sorption in a swelling polymer plate. During stage I, compressive stresses at the surface force the plate to swell mainly in the thickness direction, whereas in stage II, the plate swells freely in three directions. The tensile stresses at the plate core (which is indicated by a thin, dashed line) are relieved when the solutes reach the core. The stresses are indicated by solid arrows, and the swelling directions are indicated by broken arrows.

the core and forces it to swell. The rate at which the compressive stresses decay at the surface should, therefore, depend not only on the rate at which the solute reaches the core (diffusivity) but also on the stress-relaxation rate of the polymer. The molecular mobility and flexibility of the polymer and, therefore, the stress-relaxation rate are for many systems related to the stiffness of the polymer. Therefore, if the rate of increase of the solute surface concentration depends entirely on the rate of compressive stress relaxation at the surface, τ_c would be a function of E. More precisely, the ability of the polymer to restrict swelling induced by the solute should correlate with the polymer bulk modulus (K). However, if Poisson's ratio varies only mildly with the stiffness of the fluoropolymers considered here, the trend would be approximately the same whether E or K was used. Figure 9 indeed shows that τ_c increased with increasing E. The same trend was observed when τ_c was plotted against the yield stress (σ_y; Fig. 9). This was not surprising because E and σ_y were correlated for these polymers (Fig. 10).

In a study of water diffusion in a hydroxyl-terminated hyperbranched polymer, it was found that it was possible to use data of the mechanical stress-relaxation time (τ_m) to describe the surface-concentration stress-relaxation time.[8] This was somewhat surprising because τ_c should be a function of both the mechanics of the polymer (τ_m) and the diffusion rate of

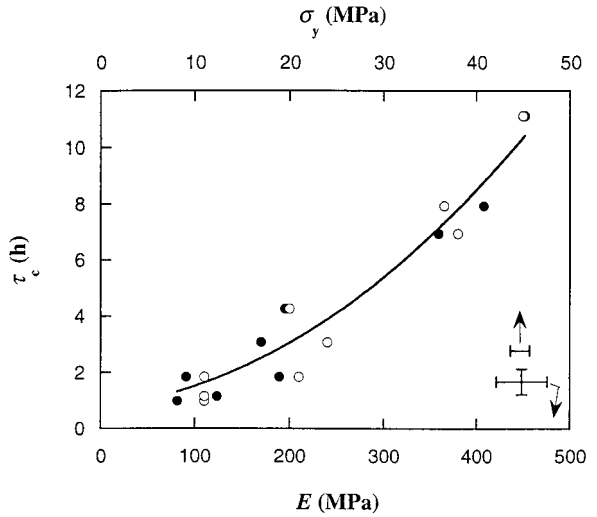

Figure 9 τ_c as a function of (●) E and (○) σ_y. The line has been drawn to show the trend.

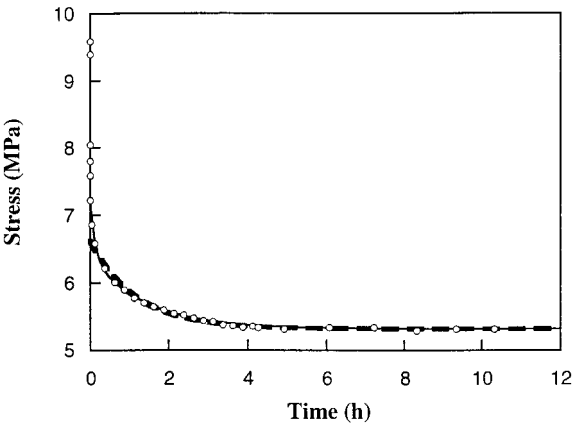

Figure 11 Mechanical stress as a function of time at 70°C for (○) ETFE. The thin, solid line represents the best fit of a three-term Prony exponential, and the thick, broken line represents the best fit of the lower part of the experimental curve with a single exponential.

the solute. The finding showed, however, that solute diffusion and mechanical relaxation were closely interrelated. Solute diffusion is limited partly by the rate of rearrangement of polymer chain segments, which, in turn, is partly dependent on the plasticization effect induced by the penetrating solute molecules. Even though it was more difficult to determine τ_m than the modulus, it was still interesting to see what the correlations were between τ_m and τ_c in the case of TCE sorption in the fluoropolymers. As was the case with the hydroxyl-terminated hyperbranched polymer, it was possible to fit the complete mechanical stress-relaxation curve by a Prony series[8] consisting of three exponential terms corresponding to three relaxation times (τ_m; Fig. 11). However, for comparison with eq. (7), a single exponential with a single τ_m value was fit to the lower part of the mechanical relaxation curve, that is, the part that could be visually separated from the y axis. It was thought that the rapid decrease in stress at the onset of stress relaxation was connected to the initial solute sorption (C_i) rather than the subsequent slow approach to C_∞. Figure 12 shows that τ_c was larger than τ_m for the majority of the data. A possible explanation is that, at 70°C in this system, solute diffusion is slower than polymer-segment relaxation. The rate of compressive stress relaxation at the surface and, therefore, τ_c, would be limited initially by the time for the solute to reach the core. The good correlation between τ_c and τ_m in the water-hyperbranched polymer system[8] existed because τ_c was primarily controlled by the polymer molecular flexibility and not by the rate of solute diffusion.

It would be desirable, for the fitting of sorption curves, to be able to assess τ_c independently, that is, from sources other than the sorption data. This would limit the number of fitting parameters and, therefore, facilitate the calculation of diffusivity parameters from the sorption experiment. An attempt was made to find

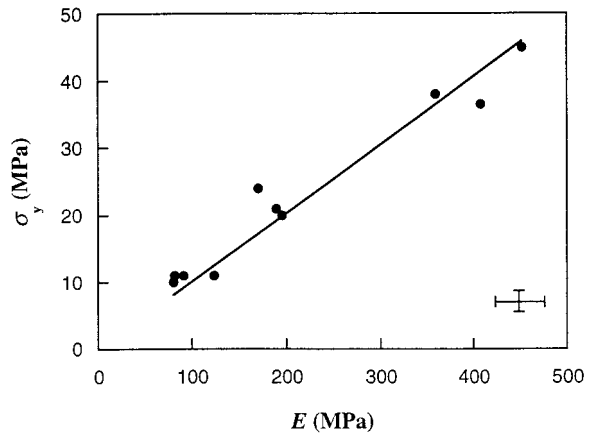

Figure 10 σ_y as a function of E. The line represents the best linear fit of the data.

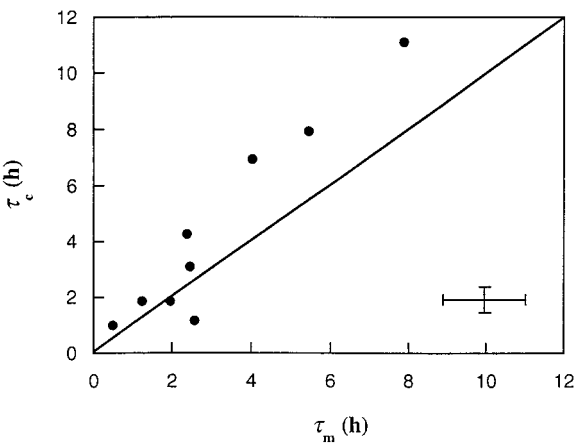

Figure 12 (●) τ_c as a function of τ_m. The line represents the equivalence curve.

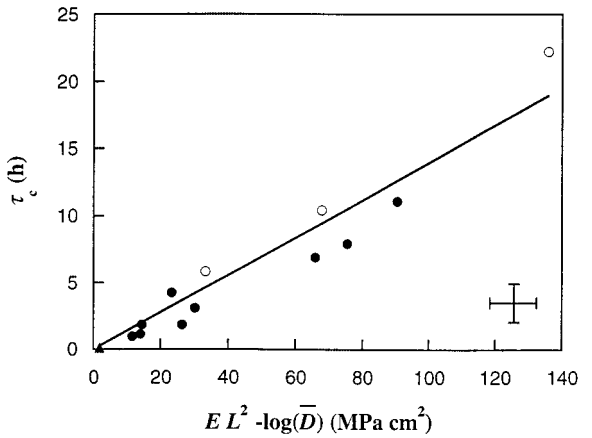

Figure 13 τ_c as a function of the product of the dry polymer value of E, L^2, and the negative of the logarithm of $\bar{D}$ (cm^2/s): (●) TCE/fluoropolymers, (▲) water/hyperbranched polymer,[8] and (○) limonene/high-density polyethylene.[26] The line represents the best linear fit of the data.

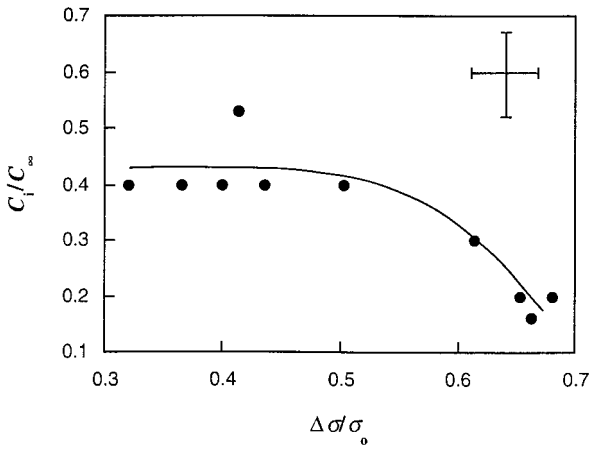

Figure 15 Relative initial solute surface concentration (C_i/C_∞) as a function of the stress-relaxation strength ($\Delta\sigma/\sigma_0$) of the fluoropolymers. The line has been drawn to show the trend.

a correlation between τ_c and many different parameters. It turned out that the best correlation was obtained when τ_c was plotted against a term consisting of the product of E for the dry polymer, the square of the dry plate thickness (L^2), and the negative of the logarithm of the average solute diffusivity ($\bar{D}$). As shown in Figure 13, it appears that the relationship is universal; that is, data from completely different solute–polymer systems conformed to the same curve. However, more data from other systems are needed, and are currently being obtained, to validate the relationship.

It would be equally desirable, for the fitting of sorption curves, to be able to assess the C_i/C_∞ ratio independently. C_i/C_∞ was, therefore, also related to several parameters. C_i/C_∞ increased with increasing E (Fig. 14). Interestingly, the water-hyperbranched polymer and limonene–polyethylene systems conformed to the same trend, although the scatter was large. Moreover, the C_i/C_∞ ratio decreased with increasing stress-relaxation strength ($\Delta\sigma/\sigma_0$; Fig. 15). Unfortunately, it was not possible to check whether other systems conformed to this trend because of the lack of data.

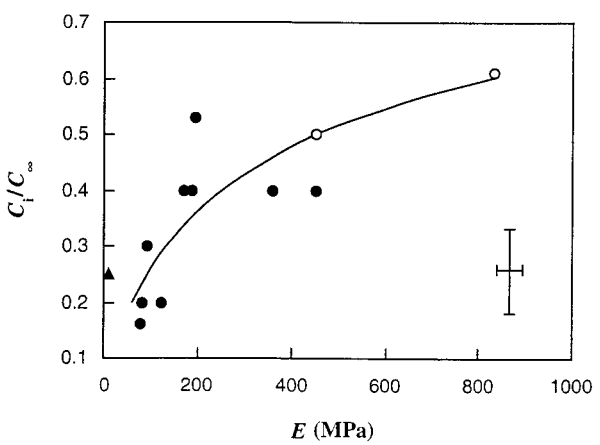

Figure 14 Relative initial solute surface concentration (C_i/C_∞) as a function of E: (●) TCE fluoropolymers, (▲) water-hyperbranched polymer,[8] and (○) limonene/high-density polyethylene.[26] The line has been drawn to show the trend.

CONCLUSIONS

The transport properties were dependent on both the chemical structure and crystallinity of the polymer. However, the chemical structure seemed to be the most important factor and could be rationalized in terms of the Hansen solubility parameters. The effects of the degree of crystallinity on the transport properties were important within each fluoropolymer group. The TCE D_{co} value decreased linearly with increasing crystallinity within the PVDF series and within the pure and modified PTFE (PTFE/PFA/MFA) series. The highest permeability was observed in the dipole-containing ECTFEs because of their high TCE solubility. The lowest permeability was observed in the hydrogen-bonding PVDF polymers because of the combination of their low solute solubility and solute diffusivity. The solute-surface-concentration stress-relaxation time correlated universally with the product of E, L^2, and $-\log(\bar{D})$. In addition, the ratio of the initial surface solute uptake to the final surface solute uptake was shown to increase with the increasing stiffness of the polymer. The water-hyperbranched polymer and limonene–polyethylene systems conformed to the same trend.

Patrizia Maccone and Matteo Vecellio at Ausimont S.p.A. (Italy) are thanked for their assistance with the experiments, and Ulf W. Gedde at the Department of Fibre and Polymer Technology is thanked for his valuable comments.

References

1. Conde, M.; Bergman, G. Swedish Corrosion Institute: Stockholm, 1996; p 1.
2. Conde, M. Swedish Corrosion Institute: Stockholm, 1997; p 1.
3. Lee, S.; Knaebel, K. S. J Appl Polym Sci 1997, 64, 477.
4. Lee, S.; Knaebel, K. S. J Appl Polym Sci 1997, 64, 455.
5. Hedenqvist, M. S.; Gedde, U. W. Polymer 1999, 40, 2381.
6. Maccone, P.; Brinati, G.; Arcella, V. Polym Eng Sci 2000, 40, 761.
7. Crank, J. The Mathematics of Diffusion; Clarendon: Oxford, 1986.
8. Hedenqvist, M. S.; Yousefi, H.; Malmström, E.; Johansson, M.; Hult, A.; Gedde, U. W.; Trollsås, M.; Hedrick, J. L. Polymer 2000, 41, 1827.
9. Hedenqvist, M.; Gedde, U. W. Prog Polym Sci 1996, 21, 299.
10. Hedenqvist, M. S.; Angelstok, A.; Edsberg, L.; Larsson, P. T.; Gedde, U. W. Polymer 1996, 37, 2887.
11. Cohen, M. H.; Turnbull, D. J Chem Phys 1959, 31, 1164.
12. Fujita, H. Fortschr Hochpolym Forsch 1961, 3, 1.
13. Hedenqvist, M. S.; Ohrlander, M.; Palmgren, R.; Albertsson, A.-C. Polym Eng Sci 1998, 38, 1313.
14. Long, F. A.; Richman, D. J Am Chem Soc 1960, 82, 513.
15. Rossi, G. Trends Polym Sci 1996, 4, 337.
16. Hedenqvist, M. S.; Krook, M.; Gedde, U. W. Polymer 2002, 43, 3061.
17. Kerbow, D. L.; Sperati, C. A. In Polymer Handbook; Brandrup, J.; Immergut, E. H.; Grulke, E. A., Eds.; Wiley: New York, 1999; Vol. 31.
18. Wunderlich, B. Macromolecular Physics; Academic: New York, 1980.
19. Khanna, J. P.; Turi, E. A.; Sibilia, J. P. J Polym Sci Polym Phys Ed 1984, 22, 2175.
20. Wunderlich, B. ATHAS Databank. http://www.web.utk.edu/~athas/databank.
21. Hansen, C. M. Hansen Solubility Parameters: A Users Handbook; CRC: Boca Raton, FL, 2000.
22. Hedenqvist, M. S.; Johnsson, G.; Tränkner, T.; Gedde, U. W. Polym Eng Sci 1996, 36, 271.
23. Bakhouya, A.; Brouzi, A. E.; Bouzon, J.; Vergnaud, J. M. Plast Rubber Comp Proc Appl 1993, 19, 77.
24. Guerra, G.; Venditto, V.; Natale, C.; Rizzo, P.; Rosa, C. D. Polymer 1998, 39, 3205.
25. Krevelen, D. W. V. Properties of Polymers; Elsevier: Amsterdam, 1990.
26. Marklund, E.; Hedenqvist, M. S., unpublished data.